Canadian Science Publishing | Canadian Journal of Fisheries and Aquatic Sciences

A spatial-temporal approach to modeling somatic growth across inland recreational fisheries landscapes

Journal:	*Canadian Journal of Fisheries and Aquatic Sciences*
Manuscript ID	cjfas-2019-0434.R2
Manuscript Type:	Article
Date Submitted by the Author:	03-Jul-2020
Complete List of Authors:	Cahill, Christopher; University of Calgary, Department of Biological Sciences Anderson, Sean; Fisheries and Oceans Canada - Pacific Biological Station, ; Paul, Andrew; Alberta Ministry of Environment and Parks, Fish and Wildlife Policy MacPherson, Laura; Alberta Fish and Wildife, Fisheries Branch Sullivan, Michael; Alberta Fish and Wildife, Fisheries Branch van Poorten, Brett; Ministry of Environment and Climate Change Strategy, Walters, Carl; University of British Columbia, Institute for the Oceans and Fisheries Post, John; University of Calgary, Biological Sciences
Keyword:	Walleye, Density-Dependent Growth, Spatio-temporal modeling, FISHERY MANAGEMENT < General, Inland Recreational Fisheries
Is the invited manuscript for consideration in a Special Issue? :	Not applicable (regular submission)

A Spatial-temporal Approach to Modeling Somatic Growth Across Inland Recreational Fisheries Landscapes

CHRISTOPHER L. CAHILL*[1]

SEAN C. ANDERSON[2], ANDREW J. PAUL[3], LAURA MACPHERSON[4], MICHAEL G. SULLIVAN[4], BRETT VAN POORTEN[5,6], CARL J. WALTERS[6], and JOHN R. POST[1]

1. *Department of Biological Sciences, University of Calgary, Calgary, Alberta, T2N 1N4, Canada*

2. *Pacific Biological Station, Fisheries and Oceans Canada, 3190 Hammond Bay Road Nanaimo, British Columbia, V6T 6N7, Canada*

3. *Fish and Wildlife, Alberta Environment and Parks, Provincial Building, Cochrane, Alberta, T4C 1A5, Canada*

4. *Fish and Wildlife Policy, Alberta Environment and Parks 7th Floor, O.S. Longman Building 6909 116 Street Edmonton, Alberta, T6H 4P2, Canada*

5. *British Columbia Ministry of Environment and Climate Change Strategy, 2202 Main Mall, Vancouver, British Columbia, V6T 1Z4, Canada*

6. *Institute for the Oceans and Fisheries, University of British Columbia, Vancouver, British Columbia, V6T 1Z4, Canada*

*Corresponding author: christopher.cahill@ucalgary.ca

[1]Present address: Department of Biological Sciences, University of Calgary, Calgary, Alberta T2N 1N4, Canada

Abstract—We develop a mechanistically motivated von Bertalanffy growth model to estimate growth rate and its predictors from spatial-temporal data, and compare this model's performance to a suite of commonly used mixed-effects growth models. We test these models with simulated data and then apply them to test whether concerns that high density is causing growth suppression of walleye *Sander vitreus* in Alberta, Canada are supported using data collected during 2000-2017. Simulation experiments demonstrated that models that failed to account for complex dependency structures often resulted in growth-rate estimates that were less accurate and biased low as judged by median absolute relative error and median relative error, respectively. The magnitude of this bias depended on the parameter values used for simulation. For the case study, a spatial-temporal model was more parsimonious and had higher predictive performance relative to simpler models, and did not support the slow-growing walleye hypothesis in Alberta. These findings demonstrate the importance of considering spatial-temporal correlation in analyses that rely on surveillance-style monitoring datasets, particularly when examining relationships between life-history traits and environmental characteristics.

Keywords: Walleye, density-dependent growth, spatio-temporal modeling, fishery management, inland recreational fisheries

Introduction

Inland recreational fisheries are embedded in complex social-ecological systems (see Carruthers et al. 2018), generate approximately $51 billion USD·yr^{-1} in North America (Funge-Smith 2018), and support important ecosystem services when effectively managed (Lynch et al. 2016). However, those tasked with assessing and managing inland recreational fisheries face unique challenges. For example, the status of inland recreational fisheries is often determined from snapshots of monitoring data that have been collected across space and time (e.g., Lester et al. 2003; Post 2013; Lorenzen et al. 2016a), which precludes the use of many traditional assessment methods (e.g., Hilborn and Walters 1992). Thus, a key challenge of managing lakes across landscapes is that it is impossible to carry out in-depth assessments on every lake within a jurisdiction, and hence to manage on a lake-by lake basis (Shuter et al. 1998). Consequently, ecologists often use monitoring data to relate life history traits to environmental characteristics to inform ecological processes, identify vulnerable populations, and guide management actions across landscapes (e.g., Shuter et al. 1998; Lester et al. 2014a; Wilson et al. 2019a).

Little attention has been paid to the issue that the scale at which many inland recreational fisheries operate may introduce spatial and temporal correlation to the monitoring data that management agencies collect from these systems. This is important because many landscape-scale datasets are observational in nature (Nichols and Williams 2006), and because studies conducted using such datasets need to be vigilant when inferring process from pattern as a lack of controls, interspersion of treatments, and/or missing variables can all bias inference (Hurlbert 1984). Thus, the price one pays to analyze landscape-scale data is that there exists the potential for complex correlation structures within those data, which can bias statistical and ecological inference in unexpected ways (Zuur et al. 2017).

Hierarchical modeling has emerged as a powerful tool for disentangling the ecological process of interest from uncontrolled sources of observation error (Royle and Dorazio 2008); however, such modeling has typically assumed independence among lakes or years in the context of inland recreational fisheries. For instance, many studies treat lakes as discrete grouping levels for normally distributed random effects to inform fisheries ecology and management across landscapes (e.g., Helser and Lai 2004; Tsehaye et al. 2016; Wilson et al. 2019a). Whereas lakes are often treated as independent units in mixed-effects models for computational ease, there are intuitive reasons to suspect this assumption may not always hold. For example, both the landscape-scale generalizations and social-ecological-systems approaches to inland fisheries recognize that the correct scale of assessment and management is not at the scale of the individual lake—either because of correlated biological or environmental characteristics (e.g., species productivity, primary productivity, temperature, etc; Myers et al. 1997; Shuter et al. 1998) or because angler movements and hence fish dynamics may be correlated among lakes (Post et al. 2008; Kaemingk et al. 2018). Both views imply that data collected from inland recreational fisheries may be correlated in space or time, and thus methods that account for spatial-temporal correlation may help to separate signal from noise (Cressie and Wikle 2015).

In Alberta, Canada, an 18-year province-wide monitoring dataset on walleye *Sander vitreus* provides a useful case study with which to explore the challenges of analyzing monitoring data and providing management advice in the presence of spatial-temporal correlation. Walleye are among the most widely distributed and sought-after gamefishes in North America (Bozek et al. 2011), and in Alberta high angling effort and low population productivity resulted in walleye declines and collapsed fisheries by the 1990s (Post et al. 2002). In response to these declines, managers implemented stringent regulations to reduce fishing

mortality (i.e., catch-and-release, high minimum length limits), which promoted the partial recovery of walleye in many lakes by the early 2000s (Sullivan 2003). In both January 2018 and 2020, public consultations on fisheries management practices were held throughout the province. A criticism raised by many stakeholders during these meetings was that walleye populations were overabundant and hence growing slowly, termed the Slow-growing Walleye Hypothesis (SGWH). While these criticisms were anecdotal, ample evidence of density-dependent somatic growth exists in the literature (Post et al. 1999; Lester et al. 2014b). Consequently, the SGWH is important to test because angler satisfaction is driven in part by the size of fish caught (Beardmore et al. 2014), and because it implies that managers may need to strike a balance between producing a few large and many small fish (Walters and Post 1993).

This paper addresses the challenge of analyzing landscape-scale fisheries data in the presence of spatial-temporal correlation. To do so, we demonstrate a linkage between a commonly used somatic growth model and its underlying bioenergetics parameters. We then use this derivation to motivate a spatial-temporal hierarchical growth model and compare it to a suite of simpler mixed-effects models using simulated data where truth is known, and we measure model performance using several performance measures and a decision analysis. Finally, we demonstrate the unpredictable outcomes that can occur when ignoring spatial-temporal dependency by applying each of these methods to an 18-year dataset to test the SGWH in Alberta. This comparison between simulation experiment and case study application helps demonstrate the potential pitfalls of mis-specifying mixed effects models when analyzing landscape-scale fisheries datasets.

Materials and Methods

Bioenergetics Derivation of the von Bertalanffy Growth Model

The von Bertalanffy growth model is often used by fisheries managers to report fish growth patterns and can be used to test for the effects of covariates on growth rate early in life (Shuter et al. 1998). This growth model is derived from a bioenergetics model specifying

$$\frac{dW}{dt} = HW_t^{\frac{2}{3}} - mW_t. \quad (1)$$

where W is weight at time t, and H and m are mass-specific anabolic (building tissue) and catabolic (breaking down tissue) terms, respectively. Solving eqn. 1 and transforming from weight to length yields the von Bertalanffy growth function:

$$\hat{l}_i = l_\infty\left(1 - e^{(-(K)(a_i - t_0))}\right). \quad (2)$$

where a_i and $\hat{l}_i$ are the age and predicted length of fish i, respectively, l_∞ is a parameter that represents the average asymptotic maximum length of fish, K is the unitless Brody 'growth' coefficient, and t_0 is a nuisance parameter that describes age when length is hypothetically zero. This growth model implies that

$$l_\infty = \frac{H}{m} * \alpha^{-\frac{1}{3}} \quad (3)$$

where α is the shape parameter from a weight-length relationship ($W = \alpha \cdot Length^{\beta}$; see van Poorten and Walters 2015 eqs 1-6). Furthermore, it can be shown that

$$K = \frac{m}{3}. \quad (4)$$

Thus, it is commonly recommended that studies examining the effect of food availability on growth should focus primarily on l_∞ rather than K when using the von Bertalanffy growth model because l_∞ is related to the anabolic parameter H whereas K is not (e.g., Walters and Post 1993; van Poorten and Walters 2016). However, a reparameterization of the von Bertalanffy growth

model introduces a new parameter $\omega = K \cdot l_\infty$, which represents the growth rate of length measurement units·yr^{-1} in early life and reduces correlation among parameters (Gallucci and Quinn 1979). Combining eqns 3-4 to recast ω in terms of the underlying bioenergetics relationships shows that

$$\omega = \frac{H * \alpha^{-\frac{1}{3}}}{3}. \quad (5)$$

Thus, growth rate in early life is exclusively a function of anabolic gains, which scales with feeding rate or food availability (Beverton and Holt 1957 p. 105-106; Charnov 2010). Additionally, positive covariation between H and m implies that l_∞ varies much less with changes in H than would be expected if H and m were independent. Furthermore, while anglers may not care about growth in early life history per se, they do care about the size of their catch (Beardmore et al. 2014), and variation in adult size is linked to growth rate in early life (Lester et al. 2004). Consequently, we focus on ω as a proxy for food intake and density-related effects throughout this paper.

Mixed-effects von Bertalanffy Growth Models

Here we develop four mixed-effects versions of the von Bertalanffy growth model derived above to use in both our simulation experiment and case study below. The Gallucci and Quinn (1979) von Bertalanffy growth model parameterization is

$$\hat{l}_i = l_\infty\left(1 - e^{\left(-\left(\frac{\omega}{l_\infty}\right)(a_i - t_0)\right)}\right)e^{\varepsilon_i}, \quad (6)$$

$$\varepsilon_i \sim \text{Normal}(0, \sigma^2).$$

where parameters are defined in the previous section. This equation also assumes that observed lengths follow a lognormal distribution with variance σ^2. A common extension to this model is to incorporate a normally distributed random effect that accounts for unstructured, among-lake heterogeneity. For simplicity, we assume this random effect influences ω rather than all parameters simultaneously.

"by-lake" Random Effects

One mixed effects parameterization of this model is

$$\omega_{\text{lake}} \sim e^{\omega_0 + \text{Normal}(0, \sigma^2_{\text{lake}})} \quad (7)$$

where lake represents a lake-specific deviation from the global intercept ω_0 and σ^2_{lake} describes the variance in the lake-specific deviations. This "by-lake" random-effects structure is often employed in inland fisheries to assess growth and infer ecological processes from data collected across multiple lakes (see related models in Ogle et al. 2017; Wilson et al. 2019a; Höhne et al. 2020), and represents our first model.

"by-time" Random Effects

A second version of the von Bertalanffy growth model is:

$$\omega_{\text{year}} \sim e^{\omega_0 + \text{Normal}(0, \sigma^2_{\text{year}})} \quad (8)$$

where year represents a year-specific deviation from the global average ω_0, and σ^2_{year} now describes the variance of the year-specific deviations. This "by-time" model applies a single deviation to the average growth rate across all lakes at each timestep (see related random effects structures in Matthias et al. 2018; Pedersen et al. 2018). The "by-time" model serves as an intermediate step between the "by-lake" model and the following model.

"both" Lake and Time Random Effects

A third "both" model features lake-specific random effects and year-specific random effects, and thus is more complex than either of the previous two mixed effects models:

$$\omega_{\text{lake,year}} = e^{\omega_0 + \text{Normal}(0, \sigma^2_{\text{lake}}) + \text{Normal}(0, \sigma^2_{\text{year}})}, \quad (9)$$

Extensions of this third "both" model have also appeared in the literature (see related models in Wagner et al. 2007; Tsehaye et al. 2016; Embke et al. 2019). The models we have noted thus far assume that the random-effect deviations are independent for lakes and/or time steps.

Autoregressive lag-1 Spatial-Temporal (ar1-st) Random Effects

Next, we introduce Gaussian Random Fields (GRFs) to extend the models above to explicitly account for structured correlation or dependency in space and time. GRFs can also help account for the effect(s) of unmeasured covariates on the response variable (Zuur et al. 2017) and, to our knowledge, have not yet been applied to the von Bertalanffy growth function. A GRF is a multi-dimensional version of a Gaussian random variable defined by the expectation, variance, and covariance of a multivariate normal distribution (Cressie and Wikle 2015). Specification of a GRF determines the value of a random variable corresponding to any point in space s or space-time s,t defined on a grid (e.g., an x-y grid for spatial models or an x-y-t grid for space-time models).

One often approximates a GRF because full estimation can be impossible, particularly for spatial-temporal models and large datasets such as those collected across landscapes by fisheries management agencies. One such approximation to a GRF is the Stochastic Partial Differential Equation (SPDE) approach (Lindgren et al. 2011), which assumes that a GRF is Markovian in nature (i.e., a Gaussian Markov Random field or GMRF), and that the spatial correlation follows a Matérn covariance function (Zuur et al. 2017). The Matérn covariance function requires estimating two parameters: Matérn κ, which describes the decorrelation rate with distance, and τ

196 , which controls the variance of the spatial noise. The Matérn parameters κ and τ provide values
197 for the spatial covariance matrix $\mathbf{\Sigma}$, and then the spatial precision matrix $\mathbf{\Sigma}^{-1}$ is calculated via
198 the analytical methods in Lindgren et al. (2011). The SPDE method requires laying a "mesh"
199 across the study area, and the nodes of this mesh are then estimated as spatially correlated
200 random effects. Spatial range (defined as the distance below which spatial correlation is
201 approximately ≤ 13%) and the marginal standard deviation of the spatial process σ_0 are then
202 calculated as derived variables (Lindgren and Rue 2015):

203 (10) $$\text{spatial range} = \frac{\sqrt{8}}{\kappa}$$

204 and

205 (11) $$\sigma_0 = \frac{1}{\tau\kappa\sqrt{4\pi}}.$$

206 We can extend the von Bertalanffy modeling framework to explicitly account for first-
207 order autoregressive spatial-temporal correlation via:

208 (12) $$\omega_{s,t} = e^{\omega_0 + v_{s,t}}$$

209 where

210 (13) $$v_{s,t} = \rho v_{s,t-1} + u_{s,t},$$

211 (14) $$u_{s,t} \sim \text{GMRF}(0, \mathbf{\Sigma}),$$

212 and

213 (15) $$v_{s,t=1} \sim \text{Normal}(0, \frac{\sigma_0^2}{1-\rho^2}).$$

214 Here, $v_{s,t}$ represents correlated site s and correlated temporal t deviations for each location and
215 year. A third parameter ρ is constrained to [-1, 1] and describes autoregressive temporal
216 correlation between t independent realizations of an isotropic spatial random field $u_{s,t}$, while the

term $1-\rho^2$ enforces stationarity of the spatial-temporal random field (see separable ar1-st random effects in Cameletti et al. 2011; Blangiardo and Cameletti 2015; Zuur et al. 2017). We use s and t to distinguish between spatial-temporal correlated random effects and their independent lake and year random effect counterparts (eqns. 7-9), although we note that for our purposes lake and s correspond to the same location (i.e., a given lake) and that year and t correspond to the same moments in time (i.e., a given year). The covariance matrix $\mathbf{\Sigma}$ is obtained using the estimated parameters κ and τ via the SPDE approach of Lindgren et al. (2011). This "ar1-st" model is formulated such that random effects for ω are estimated for each lake-year combination, and this model allows growth rates at nearby points in space and/or time to be more similar than growth rates at locations further away in space and/or time. Thus, the ar1-st model relaxes the assumptions of lake and year independence assumed by the models presented above (i.e., the by-lake, by-time, and both models).

Simulation Experiment

We conducted a four-by-four factorial experiment to demonstrate the performance of each of the models described in the previous section. Each of the four models (by-lake, by-time, both, and ar1-st) were used to simulate data, and each of the four models was then fitted to each of the simulated datasets. All simulations assumed single values for both t_0 and l_∞ to simplify comparison of patterns among scenarios. For each set of simulations, we simulated a collection of 15 lakes for 10 years and sampled 20 fish from each lake-year combination. Random effects for the by-lake, by-time, and both models were simulated in the R statistical environment (eqns 7-9; R Development Core Team 2019), while Gaussian spatial-temporal fields for the ar1-st model were simulated using the GMRFlib package in C (Rue and Follestad 2003). For the ar1-st model, we drew the centroid of each lake randomly from a uniform [0,10] distribution. We

obtained fish ages within lakes by randomly sampling integers between zero and 25, and calculated lengths by then applying the corresponding random effect values and von Bertalanffy growth parameters. We then used calculated lengths to generate observed lengths by adding lognormal noise according to eqn 6. For each model and parameter combination, we generated 300 replicate datasets and then fit all four models to each replicate dataset. We recorded the marginal maximum likelihood estimate of ω_0 from each iteration and determined bias and accuracy of models by calculating the median relative error (MRE) and the median absolute relative error (MARE) across iterations for each scenario. We repeated the entire four-by-four factorial experiment nine times (i.e., 43,200 hierarchical model fits in total) to explore the effects of varying random effect parameter values on our results, and we varied values of σ_{lake}, σ_{year}, σ_o, ρ, and spatial range from low to high values. We chose parameter values to be representative of walleye life history (Table 1), and all four random effects structures considered in the simulation experiment are listed in Table 2.

In addition to the performance metrics above, we also conducted a simple decision analysis which identified the MinMax solution, which is the estimation model that resulted in the minimum value of the maximum MARE across all simulation scenarios. MinMax is a tool used in game theory and decision analysis that is useful for identifying an option (i.e., model) that is likely to perform best given uncertainty in or incorrect assumptions about the underlying dynamics of a system (McGilliard et al. 2015). Phrased differently, the MinMax solution represents the best model to use when one does not know which of the simulation scenarios most accurately reflects truth, which is likely the case in most landscape scale age-and-growth analyses. We used MARE for the MinMax calculations because it incorporates both bias and variance in a single measure (see also McGilliard et al. 2015).

Case study application to the Alberta walleye fishery

We then applied each of the models above to Alberta's standardized Fall Walleye Index Netting (FWIN) program data (Figure 1). Data were collected according to the methods in Morgan (2002). Multi-mesh gillnets were 8 panels x 7.6 m in length, set in randomly stratified locations across the 2-5 m and 5-15 m depth strata, and fished perpendicular to shore for 21-27 h during September when water temperatures were 10-15°C. Twenty-three percent of the FWIN surveys used half the standard net length but the same proportion of mesh sizes. We doubled catch rates in half nets to make them comparable to the standard nets for our effective density calculations (below). Age was estimated using fin rays or otoliths, and we excluded fin ray age estimates > six (Koenigs et al. 2015). Sex was determined via inspection of the gonads, and we retained lakes with a minimum of 50 age-length samples for analysis. A total of 251 FWIN surveys were conducted in 81 lakes during 2000-2017 (surveys per lake: min = 1, median = 3, max = 12), and 36,798 fish were included in the analysis (18,264 females; 18,534 males).

We extended the estimation model from the simulations to incorporate fixed effects to test the SGWH in Alberta. We estimated the degree to which ω was related to intraspecific effective density, growing degree days > 5°C (GDD), interspecific effective density, and an interaction term between intra- and interspecific density:

$$\omega = e^{\omega_0 + \beta_1 \text{intra} + \beta_2 \text{GDD} + \beta_3 \text{inter} + \beta_4 \text{interaction}} \quad (16)$$

plus the random effect structures in the by-lake, by-time, both, or ar1-st models. We used the intraspecific effective-density covariate and its corresponding 95% confidence intervals from these models as our test of the SGWH in Alberta. We used average effective density as our measure of density because it strikes a balance between the number and consumption allometry

of fish in a population and thus is a more appropriate measure of density-related effects on fish growth compared to biomass or numbers per hectare (Post et al. 1999). Effective density is defined as the sum of squared fish lengths (i.e., $\sum_{i=1}^{n} \text{length}^2$). This index approximates population consumption of prey, and therefore represents the best measure of the intensity of exploitative competition (Walters and Post 1993; Post et al. 1999) . We calculated average effective density for each lake-year combination as this value divided by the number of nets set in a given lake in a given year. We used all remaining covariates to explore additional variables known to influence walleye growth rate. We estimated GDD based on the latitude, longitude, and elevation of each lake's centroid using ClimateWNA (Wang et al. 2012), and we hypothesized this would have a positive effect on growth rate. We defined interspecific density as the effective density of all non-walleye fish within a FWIN net (see S1 for species). Additionally, we included an interaction term between intra- and interspecific density to represent the hypothesis that lakes varied in terms of their overall carrying capacity, which may alter the relationship between growth rates and intraspecific density. We included an additional covariate βSex to account for differences in asymptotic size for males and females and allowed both asymptotic size and t_0 to vary randomly by lake:

$$l_\infty \sim e^{l_{\infty global} + \beta\text{Sex} + \text{Normal}(0, \sigma^2_{lake_{l_\infty}})}, \quad (17)$$

and

$$t_0 \sim t_{0_{global}} + \text{Normal}\left(0, \sigma^2_{lake_{t_0}}\right). \quad (18)$$

Covariates were standardized prior to analysis by subtracting the mean and dividing by two times the standard deviation (Gelman 2008). We fit models with Restricted Maximum Likelihood

(REML) and Maximum Likelihood (ML) to facilitate comparison among models with different random effect structures and fixed effects, respectively (Pinheiro and Bates 2006). We also fit models with and without the interaction term to simplify comparisons among models.

We used R-INLA to construct a mesh required for the SPDE approximation (Lindgren and Rue 2015), which was laid over the study area for the ar1-st model (S2). We forced mesh nodes to coincide with lake centroids because we sought to estimate random effects for individual lakes rather than having these values be interpolated among mesh nodes using weighted averages (see Zuur et al. 2017). We tested and found results for the case study were not sensitive to choice of mesh.

We compared models using Akaike's Information Criterion (AIC) and predictive scores by conducting two cross-validation experiments to evaluate the predictive performance of our models. Cross-validation involves repeatedly splitting data into "training" and "testing" sets, where models are fitted to a training set and then used to predict the testing set. We used the fitted models to calculate the natural logarithm of the likelihood of data given the predictions for the testing set and divided this by the number of observations in the testing set to obtain a predictive score for each model. Models with the highest predictive scores were deemed most parsimonious for out-of-sample prediction (Gelman et al. 2014). We used two different cross-validation routines to test performance of our models and to safeguard against overfitting: leave-one-lake-out cross-validation, which tested for a model's ability to predict data in a new lake, and h-block cross validation, which tested how well the models predicted blocks of data in space (Roberts et al. 2017).

Even more mixed effects models: random slopes ar1-st model

In addition to our primary test of the SGWH using the random-intercept models above, we conducted an additional test of this hypothesis that allowed the intraspecific density covariate to vary by lake. We note that while most inland recreational fisheries random-effects analyses assume variants of the random-intercept model forms we described above (however see Wagner et al. 2007; Tsehaye et al. 2016; Hansen et al. 2020), experience and ecological intuition suggest that the impact of intraspecific density on walleye growth rates may vary by lake (Figure 2; see also Gelman and Hill 2007). Furthermore, this parameterization provides useful information to fisheries biologists tasked with managing specific lakes (i.e., this model provides information on the relationship between effective walleye density and growth rate for a specific lake unlike the random intercept models above). We used a within-and-among-lake parameterization to explicitly separate the effect of walleye density within a given lake from the effective density effect among lakes (see Bell et al. 2018). We constructed an additional ar1-st model to allow the intraspecific density coefficients to vary randomly by group (lake):

(19) $$\omega_{s,t} = e^{\omega_0 + \beta_1 \text{intra}-\text{among} + (\beta_2 + \varepsilon_{\text{lake}})\text{intra}-\text{within} + \beta_3 \text{GDD} + \beta_4 \text{inter}}$$

where $$\varepsilon_{\text{lake}} \sim \text{Normal}(0, \sigma^2_{\text{lake}})$$

plus the ar1-st random effects. Here, intra-among represents a lake's mean effective walleye density, intra-within is the effective walleye density centered within each lake, β_2 represents the global slope estimate for walleye density, and $\varepsilon_{\text{lake}}$ represents the random deviation from β_2 for lake-specific intraspecific density effects. Thus, while our primary test of the SGWH in Alberta was conducted using the random-intercept models above, we conducted this additional test to explore whether the SGWH was supported in any specific lake within the Alberta FWIN dataset.

Thus, for this random-slopes ar1-st model we tested whether β_2 plus the lake specific deviations for slope ε_{lake} and the corresponding 95% confidence intervals overlapped zero.

Estimation

We implemented all models in Template Model Builder (TMB; see Kristensen et al. 2015), and assessed statistical validity using methods in Zuur and Ieno (2016). TMB uses the Laplace approximation to calculate the marginal likelihood of the fixed effects conditional on the best estimates of the random effects (Skaug and Fournier 2006), and calculates the gradient of the marginal likelihood via automatic differentiation (Kristensen et al. 2015). These are then passed to the R statistical environment and optimized using maximum marginal likelihood via the nlminb() function (R Development Core Team 2019). We used the R-INLA software to develop the sparse matrices required for the SPDE approximation for the ar1-st models (Lindgren and Rue 2015), and then passed this information to TMB for estimation. We note that this was necessary because R-INLA does not support nonlinear models such as the von Bertalanffy growth model. We ensured the maximum gradient of the objective function was ≤ 0.001 and the Hessian matrix was positive-definite to test for consistency with convergence. Additionally, we encountered challenges fitting the ar1-st model to datasets simulated without spatial-temporal correlation. We placed vague penalties (i.e., priors) on both ρ and τ to improve numerical performance and overcome these issues in the simulations. The penalty for ρ was:

$$\rho \sim \text{Normal}(0, 2) \quad (20)$$

while the penalty for τ was:

$$\log(\tau) \sim \text{Normal}(0, 3). \quad (21)$$

Additionally, in situations where ρ was estimated to be 1, we set ρ = 1 and re-estimated the ar1-st model so that the fitted model passed our convergence tests. These penalties and estimation techniques were not necessary for models in the case study. All code necessary to recreate our analyses and figures (including maps) is available at https://github.com/ChrisFishCahill/walleye_growth. Polygons for our maps were taken from publicly available datasets (South 2017), and all other packages and software necessary to create our maps can be found at the link above.

Results

Simulation Results

Simulations revealed that the ar1-st model was able to recover the true value of ω_0 under most of the simulated random effects structures and parameter combinations (Figure 3). Additionally, the ar1-st model featured low bias (median MRE near zero across scenarios; S3) and demonstrated accuracy comparable to that of the data generation model as judged by MARE across most scenarios (S4). In the presence of spatial-temporal correlation, the ar1-st model was often less biased and more accurate than all other models (S3; S4), though all models performed similarly well when random effect noise was low (i.e., when σ_{lake}, σ_{year}, or σ_o were at low levels; left middle panels of Figure 3; S3; S4). Performance of all models typically decreased as ρ, random-effect noise, or spatial range increased from low to high values (i.e., rows from left to right Figure 3; S3; S4).

The four-by-four factorial experiments revealed that estimation models which omitted a source of variation in terms of the true data generation process often resulted in ω_0 estimates that were biased low; the magnitude of this bias depended on the parameter values used in the simulation (Figure 3; S3). For example, if data were simulated by lake but the by-time model was

used to estimate the simulated data, the resulting ω_0 estimates from the by-time model were generally biased low (Figure 3; S3). The opposite was also true: if data were simulated using the by-time model but estimated using the by-lake model, the resulting ω_0 marginal maximum likelihood estimates from the by-lake model were often biased low (Figure 3; S3). The both and ar1-st models were more flexible and able to partition the random-effect variation of the by-lake and by-time models and thus estimated ω_0 with low bias and accuracy comparable to that of the true model (S3; S4). This general pattern remained as the true data generation process increased in complexity. For example, the ar1-st model often performed comparably well in terms of MRE and MARE to the both model when the both model was used to generate data, but the converse was not always true as ω_0 estimates from the both model were often biased low when the ar1-stmodel was used to generate data (Figure 3; S3; S4). Results from the decision analysis showed that the ar1-st model was the MinMax solution, indicating that this model was the most robust choice across the potential axes of model misspecification considered in the simulation study (MinMax MARE values: by-lake: 13.8%; by-time: 13.0%; both: 13.1%; ar1-st: 12.8%).

Case Study Results

Despite increased complexity, the ar1-st models were more parsimonious than simpler mixed effects models as judged by Δ REML AIC scores when fit to the case study data (Table 3). Additionally, the ar1-st models featured the highest out of sample predictive performance for both leave-one-lake-out and spatial h-block cross validation scores (Table 3). Comparisons of Δ ML AIC scores between models with and without interaction terms showed that the ar1-st model did not support inclusion of the interaction term, while Δ ML AIC scores for simpler models did support the inclusion of an interaction term between intra- and interspecific effective density.

The top-ranked model as determined by both AIC values and cross validation scores was the ar1-st model without an interaction term (Table 3; Figure 4; see S5 for 251 lake-year fits to data). This model estimated that female walleye grew to an $l_{\infty global}$ of 60.1 cm (CI: 58.2-61.9 cm) vs. 55.1 cm for males (CI: 53.4-56.7 cm), while $t_{0global}$ was -0.95 yr (CI: -1.03 to -0.88 yr). The global intercept for ω was 14.4 cm·yr^{-1} (CI: 13.4-15.5 cm·yr^{-1}), and lake- and year-specific growth rates estimated using the ar1-st model ranged from 7.9 to 26.3 cm·yr^{-1} (Figure 5; S5). The top ranked model indicated that the SGWH was not supported in Alberta (point estimate: 0.03; CI: - 0.01-0.07), and none of the parameters hypothesized to affect ω were significantly different from zero (Figure 6). This model also estimated that the spatial range of correlation among lakes was 52 km (95% confidence interval (CI): 41-63 km), and that ρ was 0.93 indicating there was high temporal persistence in the spatial-temporal field (CI: 0.90-0.95). Similarly, the ar1-st model with random slopes also supported the conclusions of the top ranked model. The within-lake regression coefficient for intraspecific density using the random slopes model was 0.03 (CI: -0.09-0.14), and lake-specific estimates of the relationship between walleye growth rate and intraspecific density indicated that the SGWH was not supported in any of Alberta's lakes using FWIN data collected during 2000-2017 (Figure 7). We present residual diagnostic plots for the top ranked ar1-st model in S6 and S7.

Comparison of the by-lake and ar1-st Models in the Case Study

Given the prevalence of the by-lake model in the literature, we also compared key parameter estimates and 95% confidence intervals from this model to values from the top-ranked ar1-st model. Estimates and uncertainty intervals for ω_0 from the by-lake model were shifted lower relative to the corresponding values from the ar1-st model (left panel, Figure 6). These two models also differed in terms of the SGWH test (second panel, Figure 6), and the by-lake model

tended to provide point estimates that were farther from zero relative to the ar1-st model (right four panels; Figure 6). The by-lake model also tended to estimate narrower 95% confidence intervals for parameters thought to influence growth rate relative to the ar1-st model (right four panels; Figure 6).

Discussion

We have shown how growth rate in early life—as per the von Bertalanffy growth function—is linked to anabolism, and then used this derivation to motivate a general model that estimates growth rate and its predictors from landscape-scale data with spatial-temporal correlation. Additionally, we demonstrated via simulation that this first-order autoregressive spatial-temporal (ar1-st) von Bertalanffy growth model provided superior growth rate estimates relative to a suite of simpler mixed effects models when spatial-temporal correlation was present in the data. Borrowing a tool from decision analysis, we also showed the ar1-st model was most likely to minimize the worst errors in situations when one does not know the underlying random effects structure of a given dataset. Notably, our simulation experiments also revealed that failure to specify a random effects structure that was flexible enough to capture the underlying complexity of the simulated data both decreased accuracy of growth rate estimates and resulted in estimates that were biased low relative to true values. Furthermore, for a landscape-scale case study on Walleye in Alberta we demonstrated that the ar1-st growth model vastly outperformed several simpler mixed effects models in terms of both parsimony and out-of-sample prediction performance. Lastly, the ar1-st model found no evidence of density dependent growth in the Alberta Walleye case study, which contrasted the conclusions obtained from the simpler by-lake mixed effects von Bertalanffy growth model and the claims of some anglers in the province. We explore these findings and their implications in detail below.

An important result from our simulations was that unmodeled dependency in mixed effects von Bertalanffy growth models often results in growth rate estimates that are biased low; however, this bias largely disappeared when using the ar1-st growth model that explicitly accounted for complex random effects structures. We suggest this bias is related to a lack of independence (presence of pseudoreplication) in the simulated data, which increases both parameter bias and the type I error rate in regression models when not accounted for (Hurlbert 1984; Zuur and Ieno 2016). Furthermore, we speculate that this bias is negative due to nonlinearities in the von Bertalanffy growth model. We believe our findings parallel those of Miller et al. (2018), who showed that temporal correlation inflated the effect size of covariates thought to influence growth unless this source of dependency was explicitly accounted for using state-space modeling. This finding has broad implications given the prevalence of the von Bertalanffy growth model in the literature (e.g., Hilborn and Walters 1992; Walters and Essington 2010; Lee et al. 2017), the importance of obtaining accurate and reliable growth-rate estimates for both stock assessments and basic ecological research (Lorenzen et al. 2016b; Korman et al. 2017; Lorenzen and Camp 2019), and because the simpler hierarchical models we used here are often considered the *de facto* standard for analyzing age and growth data (e.g., Helser and Lai 2004; Ogle et al. 2017). Our findings demonstrate that ecologists should be wary when applying mixed effects growth models to analyze landscape-scale datasets given the near ubiquity of spatial-temporal correlation in real-world data (Cressie and Wikle 2015), and because of the challenges of determining how such correlation will impact an analysis (Zuur et al. 2017; this study). Thus, we recommend that investigations examining relationships between life-history traits such as growth and environmental characteristics explicitly incorporate the effects of space and time, and note that our findings are consistent with mounting evidence that spatial-

temporal models improve estimates of density dependence (Thorson et al. 2015b), abundance (Royle et al. 2013), species distributions (Thorson et al. 2015a), and rare or extreme ecological events (Anderson and Ward 2019).

Our results from both the top-ranked ar1-st model and the random slopes ar1-st model show that the available data do not support the conclusion that Walleye are experiencing density-dependent growth in Alberta. This is surprising given the range of densities observed due in part to the continued recovery of walleye in the province (Sullivan 2003), the wide range of growth rates we documented (e.g., see Figures 4 and 5), and numerous studies demonstrating density-dependent juvenile growth with similar datasets in other fisheries (e.g., Lester et al. 2014b; Ward et al. 2016). We expected the effects of density to be most pronounced during early life-history stages (Lorenzen and Camp 2019), and thus tested for density effects on a parameter that approximates maximum juvenile growth rate (Gallucci and Quinn 1979); however, there may be issues with this approach. First, the von Bertalanffy growth model has been criticized on theoretical grounds as it has been suggested that this model cannot cleanly separate juvenile and adult growth rates (see Rennie et al. 2008). Nonetheless, the von Bertalanffy model we implemented provided an index of juvenile growth rate in $cm \cdot yr^{-1}$, and we showed that the growth rate parameter we focused on is a consequence of tissue-building processes using simple mechanistic relationships (see also van Poorten and Walters 2016). We believe that such a first-principles approach to modeling holds great potential for gaining new insights in complex ecological systems, similar to recommendations for both population ecology and spatial-temporal modeling more generally (Brännström and Sumpter 2005; Cressie and Wikle 2015). With this in mind, future studies could adapt more complex growth models to explicitly incorporate spatial-temporal random effects using a predictive process approach (see models in

Latimer et al. 2009). Second, the approach we used treated t_0 and L_∞ as standard, lake-specific random effects instead of spatially- or time-varying quantities, which may not be warranted (Lee et al. 2017; this study). Spatial-temporal effects for these portions of the growth model were inestimable given the available data, although informative priors could be used to improve estimation of these quantities in the future. Lastly, it is possible that density dependence affects walleye in life stages other than early growth, or that density effects could interact with lifetime growth schedules in ways we did not consider (see Lorenzen and Camp 2019).

The finding that Walleye in the province were not experiencing density-dependent growth rate suppression during 2000-2017 contrasts the claims of some anglers, and we believe this discrepancy has important implications for fisheries management in Alberta. Some anglers report catching more fish than they did in the 1990s, and that many of the fish they do catch are below the harvestable size. Numerous conversations with anglers during public consultation meetings in January and February 2020 revealed that anglers often capture many sub-legal size walleye before capturing a single harvestable-size fish, and that many interpret this as evidence for slow growth rates and/or stunting; this is then used to advocate for more liberal harvest regulations (C.L. Cahill, pers. obs.). However, we explicitly tested the density-dependent growth hypothesis and showed that growth rate suppression was not supported. We suggest that it is important to remember that fishing mortality caused many accessible Walleye populations in Alberta to decline and collapse by the mid-1990s (Post et al. 2002), and that stringent regulations such as minimum length limits, catch and release, and a novel harvest lottery tool have since been used to improve Walleye abundance in many of the lakes (Sullivan 2003; Spencer 2010). Additionally, survey data in some lakes clearly show that walleye grow until they reach harvestable size and that beyond this size, length frequency histograms appear truncated. This

truncation often coincides with the minimum length limit for a given lake (see examples in Spencer 2010). We note that while harvest regulations vary by lake and year across the province, this size truncation is most apparent in several lake-years in S5 where 50 cm minimum length limits have been in place for a minimum of five years (S5; see Buck Lake 2005-2010, 2017; Iosegun Lake 2005; Round Lake 2017; Smoke Lake 2005, 2013; Sturgeon Lake 2017). This information coupled with our findings suggests that the reason anglers catch many small fish is not because those fish grow slowly or are stunted, but rather because large fish may be removed from these populations by harvest. Ironically, if harvest was increased in an attempt to improve growth rates, fish may be exposed to unsustainable levels of exploitation and decline toward population levels observed in the 1990s (see Post et al. 2002; Sullivan 2003; Spencer 2010).

Differences between the by-lake model and top ranked ar1-st model illustrate an important finding of our work: failure to account for complex correlation structures in real-world datasets can have unexpected consequences for an analysis and thus change ecological inference (see also Figure 6; Zuur et al. 2010; Cressie and Wikle 2015; Zuur et al. 2017). This is relevant given many landscape-scale inland fisheries studies often consider some variant of the by-lake model as their most complex hierarchical model (Ward et al. 2016; Rypel et al. 2018; Höhne et al. 2020). Not only were error bars from the by-lake model typically narrower than the ar1-st model, but point estimates for certain parameters also changed from negative to positive values and were typically larger in magnitude (Figure 6). Additionally, the by-lake and ar1-st models ultimately resulted in different inferences regarding the SGWH in Alberta. While we do not know the underlying "truth" in the case study, we believe it is likely that the ar1-st model provides a better appraisal of the inherent complexity and uncertainty present in the Alberta

553 Walleye dataset, particularly when considered in conjunction with our simulation findings and
554 our case-study model comparisons using AIC and cross validation.

555 From an applied perspective, disparities between the by-lake and ar1-st models could
556 result in different advice being provided to biologists and policy makers managing walleye in
557 Alberta. For example, the commonly used by-lake model indicated that size-based fisheries
558 objectives may require reductions in walleye densities through more liberal harvest regulations to
559 improve growing conditions (see arguments in Walters and Post 1993; Wilson et al. 2016). In
560 contrast, the better-supported ar1-st model showed that reducing density was unlikely to improve
561 walleye growth rates. Thus, naïve adoption of the simpler hierarchical model's results could
562 result in harvest policies not supported by the data and which could lead to overfishing. This
563 finding is noteworthy given the prevalence of datasets originating from surveillance-style
564 monitoring programs in both fisheries and applied ecological settings more generally, and
565 because such datasets are often used to inform resource management across broad spatial-
566 temporal scales (see examples in Lester et al. 2003; Nichols and Williams 2006; Cain et al.
567 2019). While decision analysis would ideally be used to guide management actions such as
568 these, we note that such analyses are rarely employed across landscapes in inland recreational
569 fisheries (see Punt and Hilborn 1997; van Poorten and MacKenzie 2020). As a result, we
570 suggest that coupling spatial-temporal methods such as those used here with decision analysis
571 and value of information modeling may represent a fruitful area for future research in inland
572 recreational fisheries (see Hansen and Jones 2008).

573 The top-ranked model as judged by AIC and cross validation indicated that walleye
574 growth rates were correlated to a spatial range of about 52 km in Alberta, and that there was high
575 temporal persistence in this spatial-temporal field. This distance is remarkably similar to results

presented in Myers et al. (1997), who showed that recruitment in freshwater fishes was spatially correlated to distances of about 50 km. These authors hypothesized that the correlation they detected in recruitment was primarily due to the effects of "planktonic patchiness" and/or predation in otherwise isolated lakes. Similarly, growth rates in our study were spatially correlated among lakes at short distances after we accounted for sex, intraspecific and interspecific effective density, and temperature even though lakes were not physically connected. The processes we modeled suggest that this residual correlation may be due in part to similarities in primary productivity and/or in how this food is partitioned among communities in nearby lakes, as both factors could govern the food supply available to walleye within a given lake and hence local growth rates. The residual spatial-temporal correlation we documented may represent a fundamental limitation, and experimentation may be necessary to further resolve our collective understanding of the remarkable variation in Walleye growth rates across this large inland recreational fishery landscape (see Figures 4 and 5; see also Walters 1986; Walters et al. 1988).

Many of the key issues in inland recreational fisheries science and management inherently require spatial-temporal thinking (e.g., see Arlinghaus et al. 2017), and yet spatial-temporal statistical techniques remain underused in the literature (however see Myers et al. 1997; Isaak et al. 2014; Hocking et al. 2018). When compared to a suite of commonly used mixed effects von Bertalanffy growth models that assumed lake and year independence, the spatial-temporal growth model introduced here provided more accurate and less biased growth rate estimates in datasets similar to those found in many applied ecological settings. Furthermore, the spatial-temporal growth model improved fits to real-world data when compared to the simpler mixed effects models, and differences in key predictions between the model types could have

599 resulted in misleading biological advice to resource managers. While this study focused on
600 nonlinear spatial-temporal growth modeling, we see several potential avenues for future
601 research. For example, questions involving spatial exploitation patterns near urban areas
602 (Wilson et al. 2019b), the effective design of landscape-scale monitoring programs or adaptive
603 management experiments (Walters 1986; Williams et al. 2018), and the examination of fish-
604 habitat relationships to inform fisheries management practices (Grüss et al. 2019) can all be
605 confronted within the modeling framework presented here. Thus, we hope that embracing the
606 spatial-temporal complexity inherent to inland recreational fisheries will result in richer
607 ecological inferences and improve policy recommendations in the future.

608 **Acknowledgements**

609 We thank the biologists and technicians involved in the FWIN program. CC
610 acknowledges critical conversations with M. Faust, G. Courtice, K. Wilson, and J. Thorson, and
611 is supported by a Vanier Canada Graduate Scholarship and a research grant from the Alberta
612 Conservation Association. D. Goethel and three anonymous reviewers improved an earlier
613 version of this manuscript.

614 **References**

615 Anderson, S.C., and Ward, E.J. 2019. Black swans in space: modeling spatiotemporal processes
616 with extremes. Ecology **100**(1): e02403.

617 Arlinghaus, R., Alós, J., Beardmore, B., Daedlow, K., Dorow, M., Fujitani, M., Hühn, D.,
618 Haider, W., Hunt, L., and Johnson, B. 2017. Understanding and managing freshwater
619 recreational fisheries as complex adaptive social-ecological systems. Reviews in
620 Fisheries Science & Aquaculture **25**(1): 1-41.

621 Beardmore, B., Hunt, L.M., Haider, W., Dorow, M., and Arlinghaus, R. 2014. Effectively
622 managing angler satisfaction in recreational fisheries requires understanding the fish
623 species and the anglers. Canadian Journal of Fisheries and Aquatic Sciences **72**(4): 500-
624 513.

Bell, A., Jones, K., and Fairbrother, M. 2018. Understanding and misunderstanding group mean centering: a commentary on Kelley et al.'s dangerous practice. Quality & quantity **52**(5): 2031-2036.

Beverton, R., and Holt, S. 1957. On the dynamics of exploited fish populations. Chapman & Hall.

Blangiardo, M., and Cameletti, M. 2015. Spatial and spatio-temporal Bayesian models with R-INLA. John Wiley & Sons.

Bozek, M.A., Baccante, D.A., and Lester, N.P. 2011. Walleye and sauger life history. Biology, management, and culture of Walleye and Sauger **233**: 301.

Brännström, Å., and Sumpter, D.J. 2005. The role of competition and clustering in population dynamics. Proceedings of the Royal Society B: Biological Sciences **272**(1576): 2065-2072.

Cain, R.L., Snow, N.P., Crawford, J.C., Williams, D.M., and Porter, W.F. 2019. Spatial distribution and landscape associations of large-antlered deer. The Journal of Wildlife Management.

Cameletti, M., Ignaccolo, R., and Bande, S. 2011. Comparing spatio-temporal models for particulate matter in Piemonte. Environmetrics **22**(8): 985-996.

Carruthers, T.R., Dabrowska, K., Haider, W., Parkinson, E.A., Varkey, D.A., Ward, H., McAllister, M.K., Godin, T., Van Poorten, B., Askey, P.J., Wilson, K.L., Hunt, L.M., Clarke, A., Newton, E., Walters, C., and Post, J.R. 2019. Landscape-scale social and ecological outcomes of dynamic angler and fish behaviours: processes, data, and patterns. Canadian Journal of Fisheries and Aquatic Sciences **76**(6): 970-988. doi:10.1139/cjfas-2018-0168.

Charnov, E.L. 2010. Comparing body-size growth curves: the Gallucci-Quinn index, and beyond. Environmental biology of fishes **88**(3): 293-294.

Cressie, N., and Wikle, C.K. 2015. Statistics for spatio-temporal data. John Wiley & Sons.

Embke, H.S., Rypel, A.L., Carpenter, S.R., Sass, G.G., Ogle, D., Cichosz, T., Hennessy, J., Essington, T.E., and Vander Zanden, M.J. 2019. Production dynamics reveal hidden overharvest of inland recreational fisheries. Proceedings of the National Academy of Sciences **116**(49): 24676-24681.

Funge-Smith, S. 2018. Review of the state of the world fishery resources: Inland fisheries. FAO Fisheries and Aquaculture Circular(C942).

Gallucci, V.F., and Quinn, T.J. 1979. Reparameterizing, fitting, and testing a simple growth model. Transactions of the American Fisheries Society **108**(1): 14-25.

659 Gelman, A. 2008. Scaling regression inputs by dividing by two standard deviations. Statistics in
660 medicine **27**(15): 2865-2873.

661 Gelman, A., and Hill, J. 2007. Data analysis using regression and multilevelhierarchical models.
662 Cambridge University Press New York, NY, USA.

663 Gelman, A., Hwang, J., and Vehtari, A. 2014. Understanding predictive information criteria for
664 Bayesian models. Statistics and computing **24**(6): 997-1016.

665 Grüss, A., Walter III, J.F., Babcock, E.A., Forrestal, F.C., Thorson, J.T., Lauretta, M.V., and
666 Schirripa, M.J. 2019. Evaluation of the impacts of different treatments of spatio-temporal
667 variation in catch-per-unit-effort standardization models. Fisheries research **213**: 75-93.

668 Hansen, G.J., and Jones, M.L. 2008. The value of information in fishery management. Fisheries
669 **33**(7): 340-348.

670 Hansen, G.J., Ahrenstorff, T.D., Bethke, B.J., Dumke, J.D., Hirsch, J., Kovalenko, K.E., LeDuc,
671 J.F., Maki, R.P., Rantala, H.M., and Wagner, T. 2020. Walleye growth declines following
672 zebra mussel and Bythotrephes invasion. Biological Invasions: 1-15.

673 Helser, T.E., and Lai, H.-L. 2004. A Bayesian hierarchical meta-analysis of fish growth: with an
674 example for North American largemouth bass, Micropterus salmoides. Ecological
675 Modelling **178**(3-4): 399-416. doi:10.1016/j.ecolmodel.2004.02.013.

676 Hilborn, R., and Walters, C.J. 1992. Quantitative fisheries stock assessment: choice, dynamics
677 and uncertainty. Reviews in Fish Biology and Fisheries **2**(2): 177-178.

678 Hocking, D.J., Thorson, J.T., O'Neil, K., and Letcher, B.H. 2018. A geostatistical state-space
679 model of animal densities for stream networks. Ecological applications **28**(7): 1782-1796.

680 Höhne, L., Palmer, M., Monk, C.T., Matern, S., Nikolaus, R., Trudeau, A., and Arlinghaus, R.
681 2020. Environmental determinants of perch (Perca fluviatilis) growth in gravel pit lakes
682 and the relative performance of simple versus complex ecological predictors. Ecology of
683 Freshwater Fish.

684 Hurlbert, S.H. 1984. Pseudoreplication and the design of ecological field experiments.
685 Ecological monographs **54**(2): 187-211.

686 Isaak, D.J., Peterson, E.E., Ver Hoef, J.M., Wenger, S.J., Falke, J.A., Torgersen, C.E., Sowder,
687 C., Steel, E.A., Fortin, M.J., and Jordan, C.E. 2014. Applications of spatial statistical
688 network models to stream data. Wiley Interdisciplinary Reviews: Water **1**(3): 277-294.

689 Kaemingk, M.A., Chizinski, C.J., Hurley, K.L., and Pope, K.L. 2018. Synchrony—An emergent
690 property of recreational fisheries. Journal of applied ecology **55**(6): 2986-2996.

691 Koenigs, R.P., Bruch, R.M., Stelzer, R.S., and Kamke, K.K. 2015. Validation of otolith ages for
692 walleye (Sander vitreus) in the Winnebago System. Fisheries Research **167**: 13-21.

693 Korman, J., Yard, M.D., and Kennedy, T.A. 2017. Trends in Rainbow Trout recruitment,
694 abundance, survival, and growth during a boom-and-bust cycle in a tailwater fishery.
695 Transactions of the American Fisheries Society **146**(5): 1043-1057.

696 Kristensen, K., Nielsen, A., Berg, C.W., Skaug, H., and Bell, B. 2015. TMB: automatic
697 differentiation and Laplace approximation. arXiv preprint arXiv:1509.00660.

698 Latimer, A., Banerjee, S., Sang Jr, H., Mosher, E., and Silander Jr, J. 2009. Hierarchical models
699 facilitate spatial analysis of large data sets: a case study on invasive plant species in the
700 northeastern United States. Ecology letters **12**(2): 144-154.

701 Lee, Q., Thorson, J.T., Gertseva, V.V., and Punt, A.E. 2017. The benefits and risks of
702 incorporating climate-driven growth variation into stock assessment models, with
703 application to Splitnose Rockfish (Sebastes diploproa). ICES Journal of Marine Science
704 **75**(1): 245-256.

705 Lester, N., Shuter, B., and Abrams, P. 2004. Interpreting the von Bertalanffy model of somatic
706 growth in fishes: the cost of reproduction. Proceedings of the Royal Society of London.
707 Series B: Biological Sciences **271**(1548): 1625-1631.

708 Lester, N.P., Shuter, B.J., Venturelli, P., and Nadeau, D. 2014a. Life-history plasticity and
709 sustainable exploitation: a theory of growth compensation applied to walleye
710 management. Ecological Applications **24**(1): 38-54. doi:10.1890/12-2020.1.

711 Lester, N.P., Shuter, B.J., Venturelli, P., and Nadeau, D. 2014b. Life-history plasticity and
712 sustainable exploitation: a theory of growth compensation applied to walleye
713 management. Ecological Applications **24**(1): 38-54.

714 Lester, N.P., Marshall, T.R., Armstrong, K., Dunlop, W.I., and Ritchie, B. 2003. A broad-scale
715 approach to management of Ontario's recreational fisheries. North American Journal of
716 Fisheries Management **23**(4): 1312-1328.

717 Lindgren, F., and Rue, H. 2015. Bayesian spatial modelling with R-INLA. Journal of Statistical
718 Software **63**(19): 1-25.

719 Lindgren, F., Rue, H., and Lindström, J. 2011. An explicit link between Gaussian fields and
720 Gaussian Markov random fields: the stochastic partial differential equation approach.
721 Journal of the Royal Statistical Society: Series B (Statistical Methodology) **73**(4): 423-
722 498.

723 Lorenzen, K., and Camp, E.V. 2019. Density-dependence in the life history of fishes: when is a
724 fish recruited? Fisheries Research **217**: 5-10.

725 Lorenzen, K., Cowx, I.G., Entsua-Mensah, R., Lester, N.P., Koehn, J., Randall, R., So, N.,
726 Bonar, S.A., Bunnell, D., and Venturelli, P. 2016a. Stock assessment in inland fisheries: a
727 foundation for sustainable use and conservation. Reviews in Fish Biology and Fisheries
728 **26**(3): 405-440.

729 Lorenzen, K., Cowx, I.G., Entsua-Mensah, R.E.M., Lester, N.P., Koehn, J.D., Randall, R.G., So,
730 N., Bonar, S.A., Bunnell, D.B., Venturelli, P., Bower, S.D., and Cooke, S.J. 2016b. Stock
731 assessment in inland fisheries: a foundation for sustainable use and conservation.
732 Reviews in Fish Biology and Fisheries **26**(3): 405-440. doi:10.1007/s11160-016-9435-0.

733 Lynch, A.J., Cooke, S.J., Deines, A.M., Bower, S.D., Bunnell, D.B., Cowx, I.G., Nguyen, V.M.,
734 Nohner, J., Phouthavong, K., Riley, B., Rogers, M.W., Taylor, W.W., Woelmer, W.,
735 Youn, S.-J., and Beard, T.D. 2016. The social, economic, and environmental importance
736 of inland fish and fisheries. Environmental Reviews **24**(2): 115-121. doi:10.1139/er-
737 2015-0064.

738 Matthias, B.G., Ahrens, R.N., Allen, M.S., Tuten, T., Siders, Z.A., and Wilson, K.L. 2018.
739 Understanding the effects of density and environmental variability on the process of fish
740 growth. Fisheries research **198**: 209-219.

741 McGilliard, C.R., Punt, A.E., Methot Jr, R.D., and Hilborn, R. 2015. Accounting for marine
742 reserves using spatial stock assessments. Canadian Journal of Fisheries and Aquatic
743 Sciences **72**(2): 262-280.

744 Miller, T.J., O'Brien, L., and Fratantoni, P.S. 2018. Temporal and environmental variation in
745 growth and maturity and effects on management reference points of Georges Bank
746 Atlantic cod. Canadian Journal of Fisheries and Aquatic Sciences **75**(12): 2159-2171.

747 Morgan, G.E. 2002. Manual of instructions: fall walleye index netting (FWIN). Percid
748 Community Synthesis, Diagnostics and Sampling Standards Working Group. Ontario.

749 Myers, R., Mertz, G., and Bridson, J. 1997. Spatial scales of interannual recruitment variations of
750 marine, anadromous, and freshwater fish. Canadian Journal of Fisheries and Aquatic
751 Sciences **54**(6): 1400-1407.

752 Nichols, J.D., and Williams, B.K. 2006. Monitoring for conservation. Trends in ecology &
753 evolution **21**(12): 668-673.

754 Ogle, D., Brenden, T., and McCormick, J. 2017. Growth estimation: growth models and
755 statistical inference. Age and growth of fishes: principles and techniques. American
756 Fisheries Society, Bethesda, Maryland: 265-359.

757 Pedersen, E.J., Goto, D., Gaeta, J.W., Hansen, G.J.A., Sass, G.G., Vander Zanden, M.J., Cichosz,
758 T.A., and Rypel, A.L. 2018. Long-term growth trends in northern Wisconsin walleye
759 populations under changing biotic and abiotic conditions. Canadian Journal of Fisheries
760 and Aquatic Sciences **75**(5): 733-745. doi:10.1139/cjfas-2017-0084.

761 Pinheiro, J., and Bates, D. 2006. Mixed-effects models in S and S-PLUS. Springer Science &
762 Business Media.

763 Post, J. 2013. Resilient recreational fisheries or prone to collapse? A decade of research on the
764 science and management of recreational fisheries. Fisheries Management and Ecology
765 **20**(2-3): 99-110.

766 Post, J., Persson, L., Parkinson, E.v., and Kooten, T.v. 2008. Angler numerical response across
767 landscapes and the collapse of freshwater fisheries. Ecological Applications **18**(4): 1038-
768 1049.

769 Post, J.R., Parkinson, E., and Johnston, N. 1999. Density-dependent processes in structured fish
770 populations: interaction strengths in whole-lake experiments. Ecological Monographs
771 **69**(2): 155-175.

772 Post, J.R., Sullivan, M., Cox, S., Lester, N.P., Walters, C.J., Parkinson, E.A., Paul, A.J., Jackson,
773 L., and Shuter, B.J. 2002. Canada's recreational fisheries: the invisible collapse? Fisheries
774 **27**(1): 6-17.

775 Punt, A.E., and Hilborn, R. 1997. Fisheries stock assessment and decision analysis: the Bayesian
776 approach. Reviews in Fish Biology and Fisheries **7**(1): 35-63.

777 R Development Core Team. 2019. R: A language and environmnet for statistical computing. R
778 Foundation for Statistical Computing, Vienna, Austria.

779 Rennie, M.D., Purchase, C.F., Lester, N., Collins, N.C., Shuter, B.J., and Abrams, P.A. 2008.
780 Lazy males? Bioenergetic differences in energy acquisition and metabolism help to
781 explain sexual size dimorphism in percids. Journal of Animal Ecology **77**(5): 916-926.

782 Roberts, D.R., Bahn, V., Ciuti, S., Boyce, M.S., Elith, J., Guillera-Arroita, G., Hauenstein, S.,
783 Lahoz-Monfort, J.J., Schröder, B., and Thuiller, W. 2017. Cross-validation strategies for
784 data with temporal, spatial, hierarchical, or phylogenetic structure. Ecography **40**(8): 913-
785 929.

786 Royle, J.A., and Dorazio, R.M. 2008. Hierarchical modeling and inference in ecology: the
787 analysis of data from populations, metapopulations and communities. Academic Press.

788 Royle, J.A., Chandler, R.B., Sollmann, R., and Gardner, B. 2013. Spatial capture-recapture.
789 Academic Press.

790 Rue, H., and Follestad, T. 2003. GMRFLib: a C-library for fast and exact simulation of Gaussian
791 Markov random fields. version 1.07. URL: http://www. math. ntnu. no/hrue/GMRFLib.

792 Rypel, A.L., Goto, D., Sass, G.G., and Vander Zanden, M.J. 2018. Eroding productivity of
793 walleye populations in northern Wisconsin lakes. Canadian Journal of Fisheries and
794 Aquatic Sciences **75**(12): 2291-2301.

795 Shuter, B.J., Jones, M.L., Korver, R.M., and Lester, N.P. 1998. A general, life history based
796 model for regional management of fish stocks: the inland lake trout *Salvelinus*
797 *namaycush* fisheries of Ontario. Canadian Journal of Fisheries and Aquatic Sciences
798 **55**(9): 2161-2177. doi:10.1139/f98-055.

799 Skaug, H.J., and Fournier, D.A. 2006. Automatic approximation of the marginal likelihood in
800 non-Gaussian hierarchical models. Computational Statistics & Data Analysis **51**(2): 699-
801 709.

South, A. 2017. rnaturalearth: World map data from Natural Earth. R package version 0.1. 0.

Spencer, S. 2010. The Increasing Prevalence of Smaller Fish in Highly Exploited Fisheries: Concerns, Diagnosis and Management Solutions.

Sullivan, M.G. 2003. Active management of walleye fisheries in Alberta: dilemmas of managing recovering fisheries. North American Journal of Fisheries Management **23**(4): 1343-1358.

Thorson, J.T., Scheuerell, M.D., Shelton, A.O., See, K.E., Skaug, H.J., and Kristensen, K. 2015a. Spatial factor analysis: a new tool for estimating joint species distributions and correlations in species range. Methods in Ecology and Evolution **6**(6): 627-637.

Thorson, J.T., Skaug, H.J., Kristensen, K., Shelton, A.O., Ward, E.J., Harms, J.H., and Benante, J.A. 2015b. The importance of spatial models for estimating the strength of density dependence. Ecology **96**(5): 1202-1212.

Tsehaye, I., Roth, B.M., and Sass, G.G. 2016. Exploring optimal walleye exploitation rates for northern Wisconsin Ceded Territory lakes using a hierarchical Bayesian age-structured model. Canadian Journal of Fisheries and Aquatic Sciences **73**(9): 1413-1433. doi:10.1139/cjfas-2015-0191.

van Poorten, B.T., and Walters, C.J. 2016. How can bioenergetics help us predict changes in fish growth patterns? Fisheries research **180**: 23-30.

van Poorten, B.T., and MacKenzie, C.J. 2020. Using Decision Analysis to Balance Angler Utility and Conservation in a Recreational Fishery. North American Journal of Fisheries Management **40**(1): 29-47.

Wagner, T., Bence, J.R., Bremigan, M.T., Hayes, D.B., and Wilberg, M.J. 2007. Regional trends in fish mean length at age: components of variance and the statistical power to detect trends. Canadian Journal of Fisheries and Aquatic Sciences **64**(7): 968-978.

Walters, C., and Essington, T. 2010. Recovery of bioenergetics parameters from information on growth: overview of an approach based on statistical analysis of tagging and size-at-age data. The Open Fish Science Journal **3**(1): 52-68.

Walters, C.J. 1986. Adaptive management of renewable resources. Macmillan Publishers Ltd.

Walters, C.J., and Post, J.R. 1993. Density-dependent growth and competitive asymmetries in size-structured fish populations: a theoretical model and recommendations for field experiments. Transactions of the American Fisheries Society **122**(1): 34-45.

Walters, C.J., Collie, J.S., and Webb, T. 1988. Experimental designs for estimating transient responses to management disturbances. Canadian Journal of Fisheries and Aquatic Sciences **45**(3): 530-538.

836 Wang, T., Hamann, A., Spittlehouse, D.L., and Murdock, T.Q. 2012. ClimateWNA—high-
837 resolution spatial climate data for western North America. Journal of Applied
838 Meteorology and Climatology **51**(1): 16-29.

839 Ward, H.G., Post, J.R., Lester, N.P., Askey, P.J., and Godin, T. 2016. Empirical evidence of
840 plasticity in life-history characteristics across climatic and fish density gradients.
841 Canadian journal of fisheries and aquatic sciences **74**(4): 464-474.

842 Williams, P.J., Hooten, M.B., Womble, J.N., Esslinger, G.G., and Bower, M.R. 2018.
843 Monitoring dynamic spatio-temporal ecological processes optimally. Ecology **99**(3): 524-
844 535.

845 Wilson, K.L., De Gisi, J., Cahill, C.L., Barker, O.E., and Post, J.R. 2019a. Life-history variation
846 along environmental and harvest clines of a northern freshwater fish: Plasticity and
847 adaptation. J Anim Ecol **88**(5): 717-733. doi:10.1111/1365-2656.12965.

848 Wilson, K.L., Foos, A., Barker, O.E., Farineau, A., De Gisi, J., and Post, J.R. 2019b. Social–
849 ecological feedbacks drive spatial exploitation in a northern freshwater fishery: A halo of
850 depletion. Journal of Applied Ecology.

851 Wilson, K.L., Cantin, A., Ward, H.G., Newton, E.R., Mee, J.A., Varkey, D.A., Parkinson, E.A.,
852 and Post, J.R. 2016. Supply–demand equilibria and the size–number trade-off in spatially
853 structured recreational fisheries. Ecological applications **26**(4): 1086-1097.

854 Zuur, A.F., and Ieno, E.N. 2016. A protocol for conducting and presenting results of
855 regression-type analyses. Methods in Ecology and Evolution **7**(6): 636-645.

856 Zuur, A.F., Ieno, E.N., and Elphick, C.S. 2010. A protocol for data exploration to avoid common
857 statistical problems. Methods in ecology and evolution **1**(1): 3-14.

858 Zuur, A.F., Ieno, E.N., and Saveliev, A.A. 2017. Spatial, Temporal and Spatial-Temporal
859 Ecological Data Analysis with R-INLA. Highland Statistics Ltd **1**.

860

861

862 **Tables**

863 TABLE 1.—Parameters used for the von Bertalanffy growth model simulation experiement.
864 Parameters with multiple values were varied individually depending on the scenario, but were
865 otherwise held at middle values.

866 TABLE 2.—Random effects structures used in the simulation experiment and in the Alberta
867 Walleye case study. σ^2_{lake} = variance of the lake-specific random effects; σ^2_{year} = variance of the
868 year-specific random effects; σ^2_0 = variance of the spatial-temporal field; ρ = temporal
869 correlation; GMRF = Gaussian Markov Random Field; $\mathbf{\Sigma}$ = covariance matrix; $v_{s,t}$ = random
870 effects correlated in space *s* and time *t*. The covariance matrix is obtained using the Matérn
871 parameters κ and τ, which are estimated using the stochastic partial differential equation
872 approach (Lindgren et al 2015).

873 TABLE 3.—Information criteria for models fitted to the Alberta Walleye data. Akaike's
874 Information Criterion (AIC) values were calculated using restricted maximum likelihood
875 (REML; for comparing among models with different random effect structures) and maximum
876 likelihood (ML; for comparing among models with and without interaction terms). Average
877 predictive scores were used for leave-one-lake-out and spatial cross-validation (LOLO CV and H
878 block CV, respectively).

879

880

881

882 TABLE 1.—Parameters used for the von Bertalanffy growth model simulation experiement.
883 Parameters with multiple values were varied individually depending on the scenario, but were
884 otherwise held at middle values.

Parameter	Description	Value
Number of Years	Number of years for which data were simulated	10
Number of Lakes	Number of simulated lakes	15
Number of Fish	Number of simulated fish per lake	20
Age Range	Range of ages	[0, 25]
l_∞	Average asymptotic maximum size	55
ω_0	Juvenile growth rate	14
t_0	Hypothetical age when length is zero	-1
σ	SD in log space of the likelihood function	0.2
σ_{lake}	SD of the lake random effects	0.2, 0.5, 0.8
σ_{year}	SD of the year random effects	0.2, 0.5, 0.8
σ_O	SD of the spatial-temporal random effects	0.2, 0.5, 0.8
ρ	Temporal correlation	0.1, 0.5, 0.9
spatial range	Distance at which spatial correlation decreases to approximately ≤ 13%	10%, 50%, 90% of grid

885

886 TABLE 2.—Random effects structures used in the simulation experiment and in the Alberta
887 Walleye case study. σ^2_{lake} = variance of the lake-specific random effects; σ^2_{year} = variance of the
888 year-specific random effects; σ^2_0 = variance of the spatial-temporal field; ρ = temporal
889 correlation; GMRF = Gaussian Markov Random Field; $\mathbf{\Sigma}$ = covariance matrix; $v_{s,t}$ = random
890 effects correlated in space *s* and time *t*. The covariance matrix is obtained using the Matérn
891 parameters κ and τ, which are estimated using the stochastic partial differential equation
892 approach (Lindgren et al 2015).

Model	Description	Random Effects Structure
by-lake	Assumes variation around growth rates in lakes is a normally distributed variable.	$\text{Normal}(0,\ \sigma^2_{\text{lake}})$
by-time	Assumes growth rates in lakes share temporal deviations which are assumed to be a normally distributed variable.	$\text{Normal}(0,\ \sigma^2_{\text{year}})$
both	Assumes growth rates in lakes vary randomly, while also sharing common temporal deviations among lakes. All random deviations are assumed to be normally distributed.	$\text{Normal}(0,\ \sigma^2_{\text{lake}})$ $\text{Normal}(0,\ \sigma^2_{\text{year}})$
ar1-st	Relaxes the assumptions of the above models and allows growth rate deviations at locations nearby in space and/or time to be more closely related than those observed at locations further away in space and/or time.	$v_{s,t} = \rho v_{s,t-1} + u_{s,t}$ $u_{s,t} \sim \text{GMRF}(0,\ \mathbf{\Sigma})$ $v_{s,t=1} \sim \text{Normal}(0, \frac{\sigma^2_o}{1-\rho^2})$

893

894 TABLE 3.—Information criteria for models fitted to the Alberta Walleye data. Akaike's
895 Information Criterion (AIC) values were calculated using restricted maximum likelihood
896 (REML; for comparing among models with different random effect structures) and maximum
897 likelihood (ML; for comparing among models with and without interaction terms). Average
898 predictive scores were used for leave-one-lake-out and spatial cross-validation (LOLO CV and H
899 block CV, respectively).

Model	Interaction term	LOLO CV	H block CV	Δ REML AIC	Δ ML AIC
ar1-st	No	4.25	4.08	0.0	0.0
ar1-st	Yes	4.25	4.08	6.9	2.0
both	No	3.69	3.68	7997.8	7993.5
both	Yes	3.70	3.68	7917.3	7906.2
by-lake	No	3.62	3.58	10011.0	10006.4
by-lake	Yes	3.63	3.58	9990.1	9978.9
by-time	No	3.57	3.58	11736.1	11727.7
by-time	Yes	3.57	3.58	11679.7	11664.2

Figures

FIGURE 1.—Distribution of known but unsampled walleye lakes in Alberta vs. walleye lakes where surveys were conducted during 2000-2017 (open vs. closed circles, respectively). Inset: location of study area in Canada. Map created in R using publicly available datasets. See methods for information on datsets.

FIGURE 2.—Caricature demonstrating the importance of allowing coefficients to vary by group (i.e., lake) in mixed effects models for landscape-scale inland recreational fisheries analyses. In the plot on the left, lake was fitted as a random intercept and thus lake specific fits (thin lines) shared a common slope with the global fit (thick line). In the plot on the right, both intercept and slope were allowed to vary by lake (thin lines). Thus, while the latter model is more complex it allows individual lakes to demonstrate neutral or even positive responses despite a negative global relationship between growth rate and effective density (thick line).

FIGURE 3.—Simulation results demonstrating the influence of random-effect structure on the estimation performance of von Bertalanffy growth models. For each panel, each model (i.e., "by-lake", "by-time", "both, and "ar1-st") was used to generate 300 datasets (data generation model indicated by x-axis groupings). All models were then fit to each replicate dataset, and distributions of the estimated growth rate ω_0 are inidcated by the point-ranges (circle: 50th quantile; inner range: 25th and 75th quantiles, outer range: 10th and 90th quantiles). Open circles indicate a match between the data generation and estimation model, while solid horizontal lines indicate the true value of ω_0. Rows of panels indicate the influence of varying parameters singly on results; thus, row one panels demonstrate the result of increasing temporal correlation ρ of the spatial-temporal field from low to high values, while values of random effect noise σ_o and spatial

correlation range were held at middle values. Note: σ_{lake} and σ_{year} were also varied from low to high values in the σ_o row, but were otherwise held at middle values (see Table 1 for values).

FIGURE 4.—Lake-year fits (n = 251) from the ar1-st model without an interaction term compared to the observed data collected during 2000-2017. The thick orange and blue lines represent the best fits for females (open circles) and males (closed circles), respectively, while thin lines represent lake- and year-specific deviations in growth for each sex. Note that dots are jittered for visualization.

FIGURE 5.—Predictions of walleye growth rate ω in $cm \cdot yr^{-1}$ through space and time as estimated by the ar1-st model using Fall Walleye Index Netting data collected during 2000-2017. Maps created in R using publicly available datasets. See methods for information on datsets.

FIGURE 6.—Comparison of key parameters (restricted maximum likelihood estimates ± 95% C.I.) estimated with the ar1-st and by-lake models using length-at-age data collected throughout Alberta during 2000-2017. Note: estimates from the first four panels were obtained from models fit without the interaction term, whereas the fifth panel was obtained from models fit with the interaction term included in the model. Solid horizontal lines indicate no effect.

FIGURE 7.—Lake-specific estimates ($\beta_2 + \varepsilon_{lake}$) and 95% confidence intervals of the effect of intraspecific effective density on walleye growth rate ω from the ar1-st random slopes model using Fall Walleye Index Netting data collected during 2000-2017.

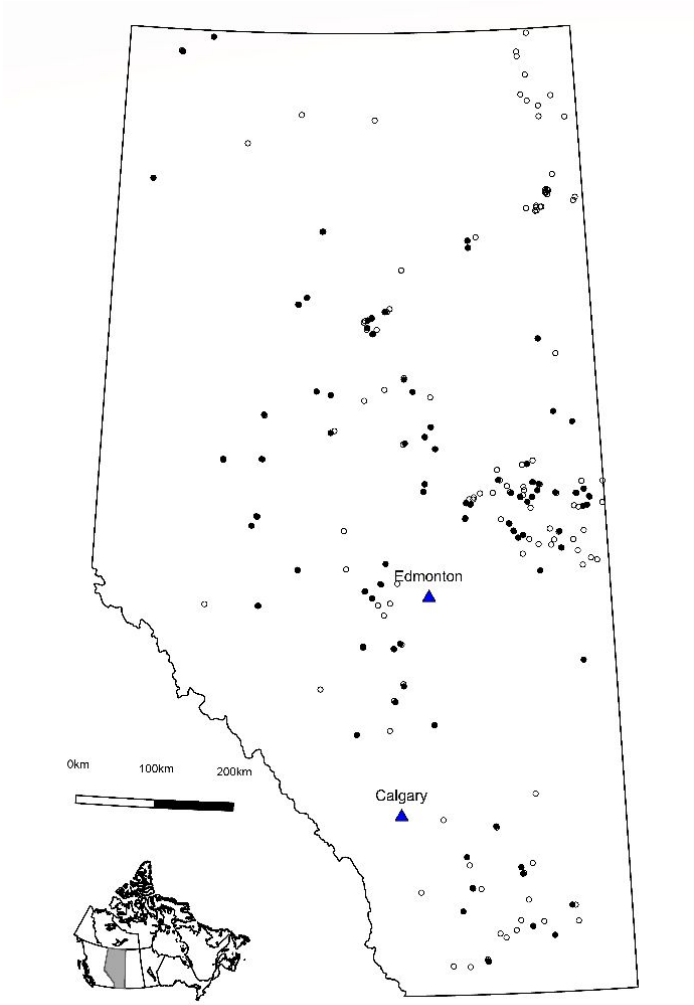

941

942 FIGURE 1.—Distribution of known but unsampled walleye lakes in Alberta vs. walleye lakes
943 where surveys were conducted during 2000-2017 (open vs. closed circles, respectively). Inset:
944 location of study area in Canada. Map created in R using publicly available datasets. See
945 methods for information on datsets.

946

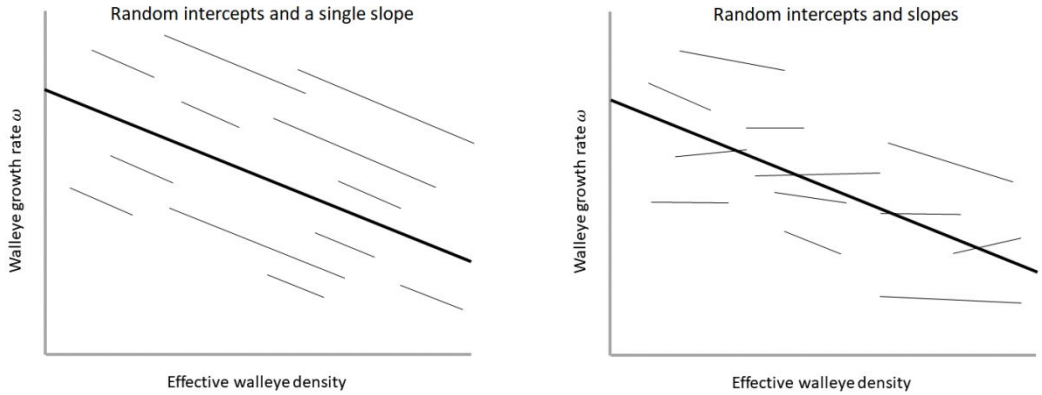

947

948 FIGURE 2.—Caricature demonstrating the importance of allowing coefficients to vary by group
949 (i.e., lake) in mixed effects models for landscape-scale inland recreational fisheries analyses. In
950 the plot on the left, lake was fitted as a random intercept and thus lake specific fits (thin lines)
951 shared a common slope with the global fit (thick line). In the plot on the right, both intercept and
952 slope were allowed to vary by lake (thin lines). Thus, while the latter model is more complex it
953 allows individual lakes to demonstrate neutral or even positive responses despite a negative
954 global relationship between growth rate and effective density (thick line).

955

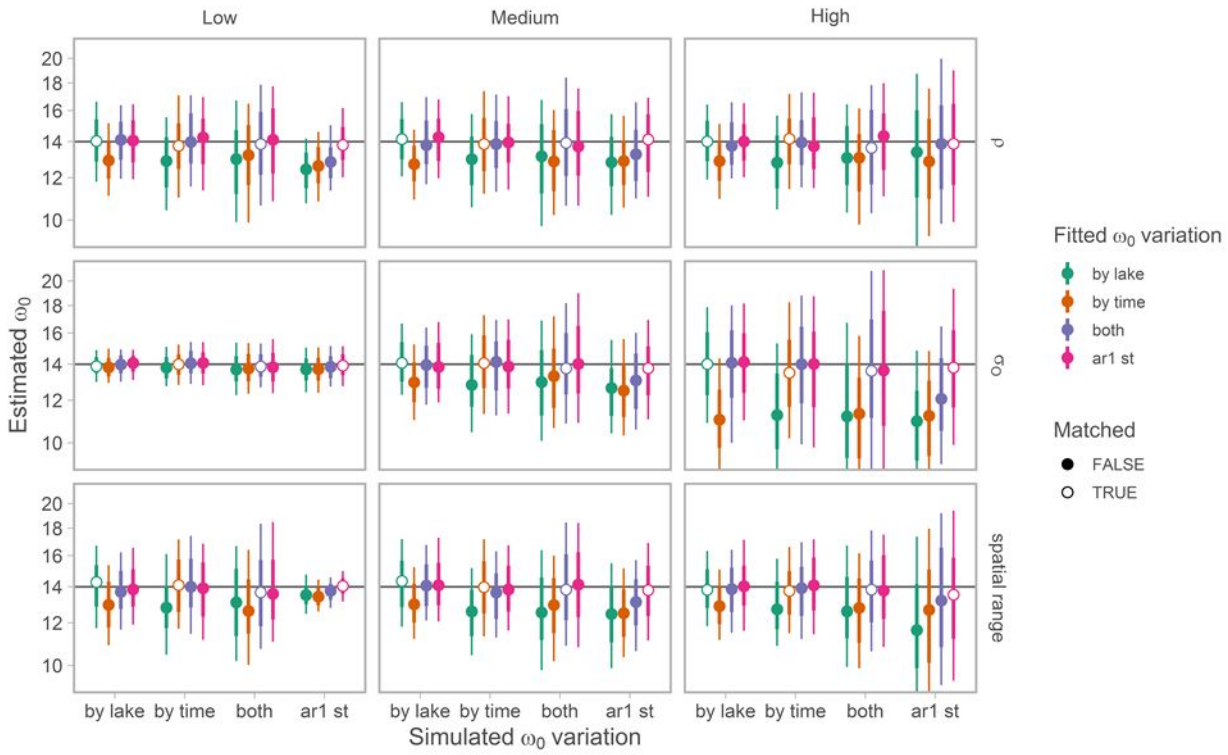

FIGURE 3.—Simulation results demonstrating the influence of random-effect structure on the estimation performance of von Bertalanffy growth models. For each panel, each model (i.e., "by-lake", "by-time", "both, and "ar1-st") was used to generate 300 datasets (data generation model indicated by x-axis groupings). All models were then fit to each replicate dataset, and distributions of the estimated growth rate ω_0 are inidcated by the point-ranges (circle: 50th quantile; inner range: 25th and 75th quantiles, outer range: 10th and 90th quantiles). Open circles indicate a match between the data generation and estimation model, while solid horizontal lines indicate the true value of ω_0. Rows of panels indicate the influence of varying parameters singly on results; thus, row one panels demonstrate the result of increasing temporal correlation ρ of the spatial-temporal field from low to high values, while values of random effect noise σ_o and spatial correlation range were held at middle values. Note: σ_{lake} and σ_{year} were also varied

968 from low to high values in the σ_o row, but were otherwise held at middle values (see Table 1 for
969 values).

970

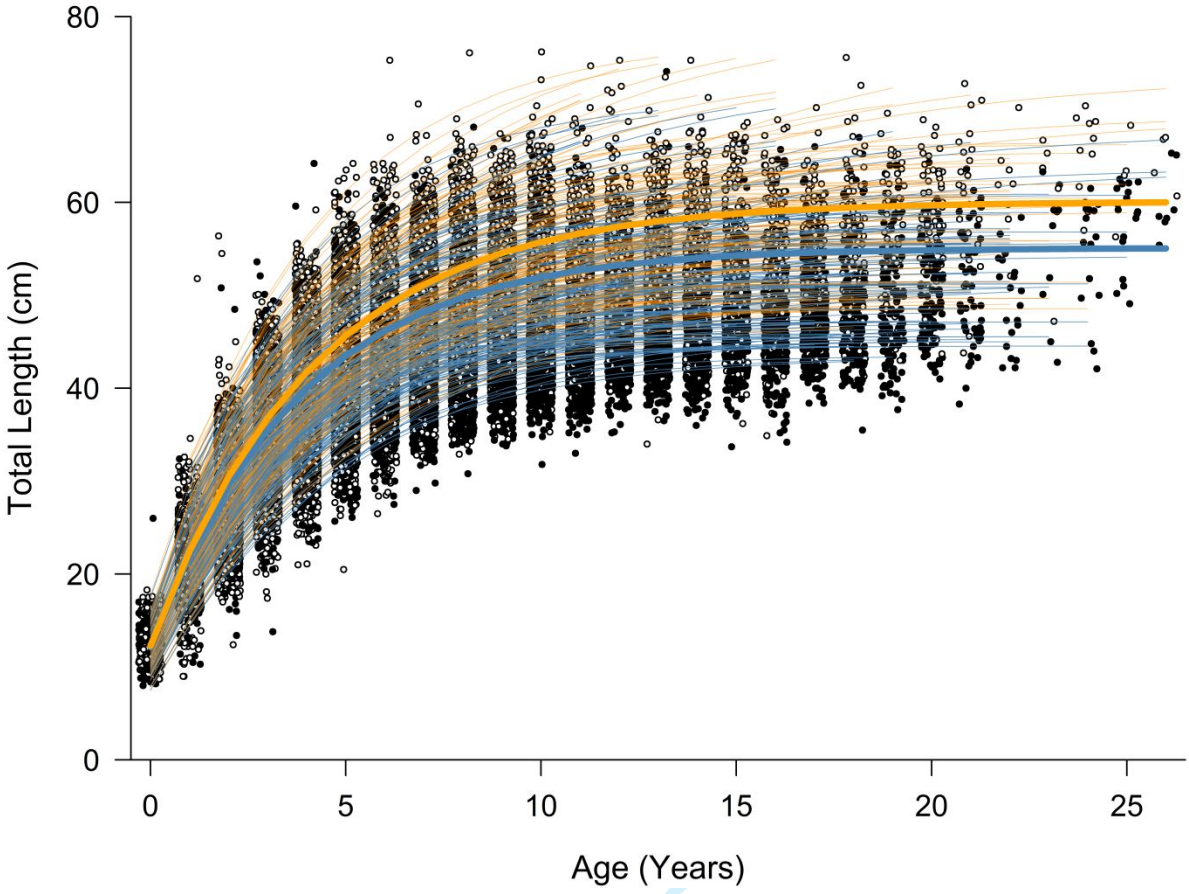

971

972 FIGURE 4.—Lake-year fits (n = 251) from the ar1-st model without an interaction term compared
973 to the observed data collected during 2000-2017. The thick orange and blue lines represent the
974 best fits for females (open circles) and males (closed circles), respectively, while thin lines
975 represent lake- and year-specific deviations in growth for each sex. Note that dots are jittered for
976 visualization.

977

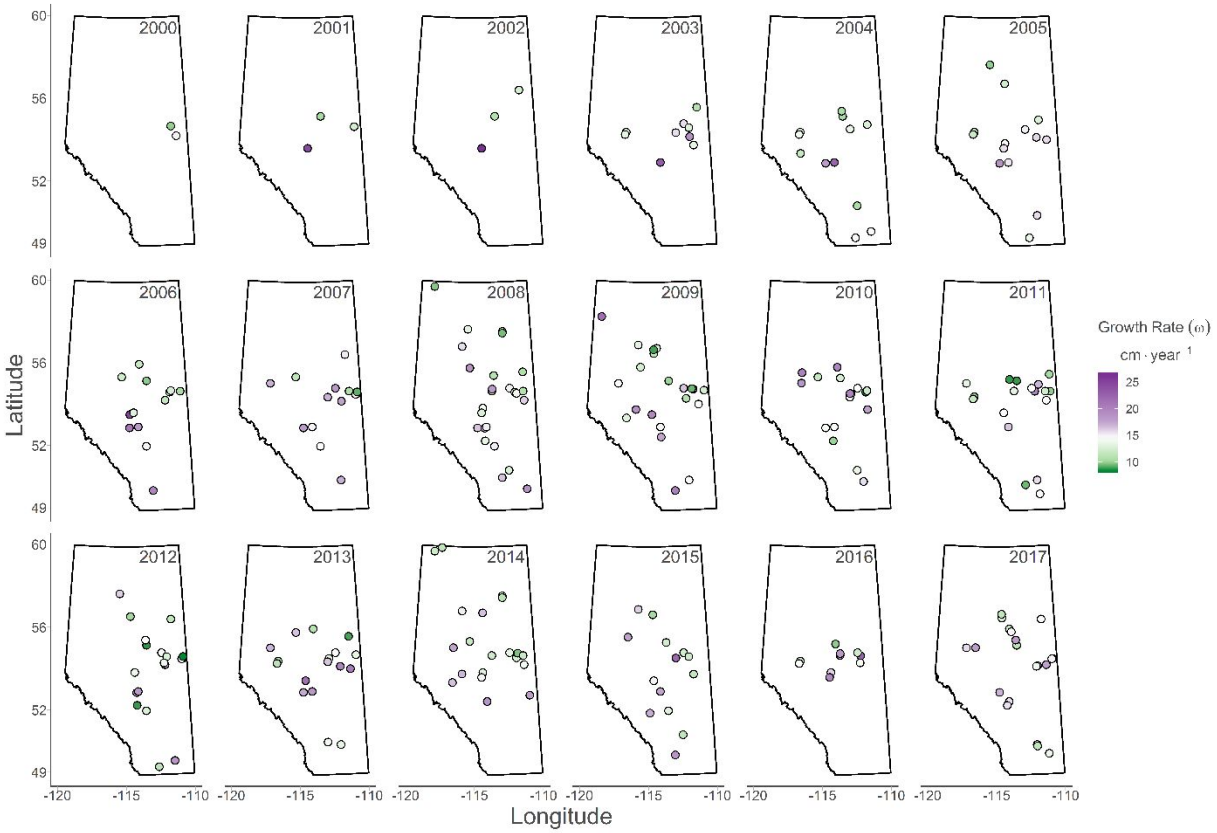

978

979 FIGURE 5.—Predictions of walleye growth rate ω in $cm \cdot yr^{-1}$ through space and time as estimated

980 by the ar1-st model using Fall Walleye Index Netting data collected during 2000-2017. Maps

981 created in R using publicly available datasets. See methods for information on datsets.

982

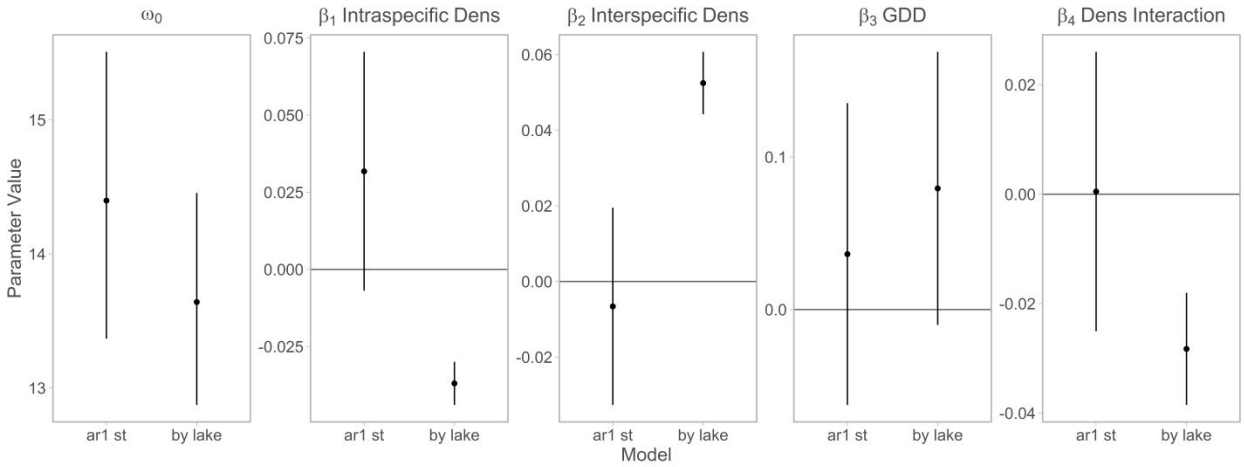

983

984 FIGURE 6.—Comparison of key parameters (restricted maximum likelihood estimates ± 95%

985 C.I.) estimated with the ar1-st and by-lake models using length-at-age data collected throughout

986 Alberta during 2000-2017. Note: estimates from the first four panels were obtained from models

987 fit without the interaction term, whereas the fifth panel was obtained from models fit with the

988 interaction term included in the model. Solid horizontal lines indicate no effect.

989

990

991 FIGURE 7.—Lake-specific estimates ($\beta_2 + \varepsilon_{\text{lake}}$) and 95% confidence intervals of the effect of

992 intraspecific effective density on walleye growth rate ω from the ar1-st random slopes model

993 using Fall Walleye Index Netting data collected during 2000-2017.

994